Neurobiology of Disease

Presenilin-1-Dependent Transcriptome Changes

Károly Mirnics,[1,2]* Zeljka Korade,[3]* Dominique Arion,[1] Orly Lazarov,[4] Travis Unger,[1] Melissa Macioce,[1] Michael Sabatini,[1,2] David Terrano,[4] Katherine C. Douglass,[1] Nina F. Schor,[3] and Sangram S. Sisodia[4]

Departments of [1]Psychiatry, [2]Neurobiology, and [3]Pediatrics, University of Pittsburgh School of Medicine, Pittsburgh, Pennsylvania 15261, and [4]Center for Molecular Neurobiology, University of Chicago, Chicago, Illinois 60637

Familial forms of Alzheimer's disease (FADs) are caused by the expression of mutant presenilin 1 (*PS1*) or presenilin 2. Using DNA microarrays, we explored the brain transcription profiles of mice with conditional knock-out of *PS1* (cKO *PS1*) in the forebrain. In parallel, we performed a transcription profiling of the hippocampus and frontal cortex of the FAD-linked ΔE9 mutant transgenic (TG) mice and matched controls [TG mice expressing wild-type human *PS1* (*hPS1*)]. When the TG and cKO datasets were cross-compared, the majority of the 30 common expression alterations were in opposite direction, suggesting that the FAD-linked *PS1* variant produces transcriptome changes primarily by gain of aberrant function. Our microarray studies also revealed an unanticipated inverse correlation of transcript levels between the brains of mice that coexpress ΔE9 *hPS1*+ amyloid precursor protein $(APP)_{695}$ Swe and ΔE9 *hPS1* single transgenic mice. The opposite directionality of these changes in transcript levels must be a function of APP and/or APP derivatives.

Key words: **presenilin; DNA microarray; Alzheimer's disease; gene expression; transcriptome; animal model**

Introduction

Presenilins are highly homologous membrane proteins that play an essential role in processing of amyloid precursor protein (APP), leading to the production of β-amyloid (Aβ) peptides (for review, see Price et al., 1998; Selkoe, 2001; De Strooper, 2003; Van Gassen and Annaert, 2003). Mutations in mutant presenilin 1 (*PS1*) and presenilin 2 (*PS2*) lead to familial forms of Alzheimer's disease (FAD) (Rogaev et al., 1995; Sherrington et al., 1995) and are characterized by enhanced production of $A\beta_{42}$ peptides (Borchelt et al., 1996; Duff et al., 1996; Scheuner et al., 1996; Borchelt et al., 1997). However, the cellular response(s) to FAD-linked *PS1* variants are not fully understood and involves simultaneous "gain of function" and "loss of function" properties (Cai et al., 2003; Marjaux et al., 2004; Saura et al., 2004).

Over the last several years, we have seen a revolution in high-throughput expression profiling of diseased human brain tissue (Ginsberg et al., 2000; Ho et al., 2001; Loring et al., 2001; Colangelo et al., 2002; Mufson et al., 2002; Yao et al., 2003; Blalock et al., 2004) and various models of human brain disorders (Dickey et al., 2003, 2004; Marcotte et al., 2003; Mirnics et al., 2003; Gan et al., 2004; Wang et al., 2004). Although the expression profiling of AD tissue continues to generate data of enormous potential, the interpretation of the postmortem findings is greatly complicated by the nature of AD disease progress (Mirnics et al., 2001a; Marcotte et al., 2003; Mirnics and Pevsner, 2004).

In an attempt to identify genes for which transcription depends on normal *PS1* function, we first performed a transcriptome profiling of the frontal cortex (FC) and hippocampus of mice with a conditional ablation of the *PS1* gene. Once we defined the gene expression pattern of the *PS1*-deficient mice, the ΔE9-mutant human *PS1* (*hPS1*) transgenic animal model attracted our attention (Lee et al., 1997; Lazarov et al., 2002). Inheritance of a single allele of *PS1* with a deletion of exon 9 results in early onset FAD in several independent pedigrees. However, because the endogenous APP production in the mouse brain is low, these mice do not develop amyloid deposits or other pathology associated with AD, and as such, may mimic the premorbid phase of human AD. As a result, data obtained in brain transcriptome profiling of ΔE9 *hPS1* mice would allow the assessment of the molecular consequences of the mutation but without the interference from cell loss or secondary transcriptome changes resulting from amyloid deposition or associated neuropathological features.

We focused our attention on the following questions in the current study. First, what are the gene expression consequences of *PS1* ablation? Second, what are the transcriptome changes that arise from expression of human ΔE9 *PS1* in mice? Third, are the genes for which expression level is modulated by conditional ablation of *PS1* also regulated in mice carrying the ΔE9 *hPS1* mutation? Finally, how do the transcriptome responses caused by expression of ΔE9 *hPS1* alone relate to those in which this polypeptide is coexpressed with the FAD-linked APP_{695} Swedish variant?

Materials and Methods

Experimental animals

Because we were interested in early transcriptome events, all transgenic animals used in the current study were killed at 3 months of age. All

Received Oct. 6, 2004; revised Dec. 10, 2004; accepted Dec. 11, 2004.

This work was supported by a National Alliance for Research on Schizophrenia and Depression Young Investigator Award (K.M.), a National Institutes of Health (NIH) Training Grant and the Pittsburgh Institute for Neurodegenerative Diseases (Z.K.), a Craumer Endowment of Children's Hospital of Pittsburgh (N.F.S.), NIH Grant AG021494 (S.S.S., O.L., D.T.), and the Ellison Medical Foundation (S.S.S., O.L., D.T.). We thank Dr. Pat R. Levitt for valuable comments on this manuscript. We also thank Carmel F. Portugal for superb technical assistance with the experiments.

*K.M. and Z.K. contributed equally to this work.

Correspondence should be addressed to either of the following: Károly Mirnics, Department of Psychiatry, University of Pittsburgh, School of Medicine, E1453 Biomedical Science, Pittsburgh, PA 15261, E-mail: karoly+@pitt.edu; or Sangram S. Sisodia, Center for Molecular Neurobiology, The University of Chicago, 947 East 58th Street, MC 0926, Chicago, IL 60637, E-mail: ssisodia@drugs.bsd.uchicago.edu.

DOI:10.1523/JNEUROSCI.4145-04.2005

Table 1. Common TG– cKO changes

Table 1A. Common TG-KO changes in opposite direction

					DE9 TRANSGENIC				CONDITIONAL KNOCKOUT				COMPARISON		
Probe	Identifier	Symbol	Chr	Name	HC	FC	ALR TG	TG p<	HC	FC	ALR KO	KO p<	HC: TG-KO	FC: TG-KO	Overall p<
1423100_at	AV026617	*Fos*	*14q24.3*	FBJ osteosarcoma oncogene	0.821	0.790	**0.8060**	**0.0074**	-0.823	-0.786	**-0.8047**	**0.0000**	Up-Down	Up-Down	*0.00001*
1448830_at	NM_013642	*Dusp1*	*5q34*	dual specificity phosphatase 1	0.755	0.815	**0.7848**	**0.0004**	-0.360	-0.349	**-0.3545**	**0.0256**	Up-Down	Up-Down	*0.00012*
1422538_at	NM_021388	*Exl2*	*1p21*	exotoses (multiple)-like 2	0.670	0.670	**0.6702**	**0.0002**	-0.304	-0.450	**-0.3767**	**0.0283**	Up-Down	Up-Down	*0.00006*
1418687_at	NM_018790	*Arc*	*8q24.3*	activity regulated cytoskeletal-associated	0.475	0.626	**0.5507**	**0.0226**	-0.746	-0.578	**-0.6620**	**0.0005**	Up-Down	Up-Down	*0.00015*
1431725_at	AK013585	*Frmn2*	*n/a*	formin 2	0.490	0.405	**0.4479**	**0.0025**	-0.311	-0.335	**-0.3228**	**0.0261**	Up-Down	Up-Down	*0.00069*
1449773_s_at	AI323528	*Gadd45b*	*19p13.3*	growth arrest/DNA-damage-inducible 45b	0.440	0.314	**0.3767**	**0.0056**	-0.229	-0.238	**-0.2332**	**0.0247**	Up-Down	Up-Down	*0.00136*
1460662_at	NM_011067	*Per3*	*1p36.23*	period homolog 3 (Drosophila)	0.321	0.408	**0.3645**	**0.0061**	-0.448	-0.352	**-0.3999**	**0.0150**	Up-Down	Up-Down	*0.00094*
1426721_s_at	BB667071	*Tiparp*	*3q25.31*	TCDD-inducible polymerase	0.247	0.433	**0.3399**	**0.0001**	-0.256	-0.374	**-0.3155**	**0.0076**	Up-Down	Up-Down	*0.00001*
1417420_at	BB538325	*Ccnd1*	*11q13*	cyclin D1	0.306	0.172	**0.2389**	**0.0243**	-0.250	-0.165	**-0.2078**	**0.0138**	Up-Down	Up-Down	*0.00302*
1427918_a_at	BI081723	*Arhq*	*2p21*	ras homolog gene family, member Q	0.127	0.291	**0.2090**	**0.0155**	-0.107	-0.397	**-0.2520**	**0.0262**	Up-Down	Up-Down	*0.00359*
1426865_a_at	BB698413	*Ncam1*	*11q23.1*	neural cell adhesion molecule 1	0.247	0.158	**0.2030**	**0.0386**	-0.197	-0.305	**-0.2511**	**0.0412**	Up-Down	Up-Down	*0.01185*
1422949_at	NM_008712	*Nos1*	*12q24.2*	nitric oxide synthase 1, neuronal	-0.300	-0.121	**-0.2106**	**0.0364**	0.170	0.254	**0.2121**	**0.0139**	Down-Up	Down-Up	*0.00434*
1449127_at	NM_009151	*Selpl*	*n/a*	selectin, platelet (p-selectin) ligand	-0.221	-0.211	**-0.2163**	**0.0001**	0.083	0.360	**0.2218**	**0.0009**	Down-Up	Down-Up	*0.00000*
1421553_at	NM_010146	*Epm2a*	*6q24*	myoclonic epilepsy, type 2 alpha	-0.237	-0.273	**-0.2549**	**0.0040**	0.484	0.354	**0.4193**	**0.0029**	Down-Up	Down-Up	*0.00014*
1417211_a_at	NM_023483	*n/a*	*n/a*	RIKEN cDNA 1110032A03 gene	-0.213	-0.342	**-0.2777**	**0.0042**	0.227	0.352	**0.2894**	**0.0135**	Down-Up	Down-Up	*0.00061*
1449401_at	NM_007574	*C1qg*	*1p36.11*	complement 1, q subcomponent, gamma	-0.342	-0.215	**-0.2785**	**0.0394**	0.162	0.541	**0.3514**	**0.0006**	Down-Up	Down-Up	*0.00028*
1455326_at	BB315720	*n/a*	*n/a*	RIKEN cDNA 4932416N17 gene	-0.317	-0.332	**-0.3245**	**0.0027**	0.090	0.341	**0.2158**	**0.0454**	Down-Up	Down-Up	*0.00123*
1425191_at	BC019407	*n/a*	*n/a*	RIKEN cDNA 9430098E02 gene	-0.350	-0.324	**-0.3366**	**0.0307**	0.202	0.414	**0.3078**	**0.0002**	Down-Up	Down-Up	*0.00008*
1418090_at	NM_032398	*Plvap*	*19p13.2*	plasmalemma vesicle associated protein	-0.411	-0.277	**-0.3441**	**0.0336**	0.379	0.355	**0.3672**	**0.0004**	Down-Up	Down-Up	*0.00016*
1451045_at	BE648447	*Syt13*	*11p12*	synaptotagmin 13	-0.405	-0.316	**-0.3603**	**0.0259**	0.358	0.425	**0.3914**	**0.0044**	Down-Up	Down-Up	*0.00115*
1417063_at	NM_009777	*C1qb*	*1p36.3*	complement 1, q subcomponent, beta	-0.383	-0.425	**-0.4042**	**0.0163**	0.318	0.708	**0.5129**	**0.0001**	Down-Up	Down-Up	*0.00002*
1423216_a_at	BM249463	*n/a*	*n/a*	RIKEN cDNA 2510049I19 gene	-0.435	-0.428	**-0.4317**	**0.0062**	0.299	0.186	**0.2422**	**0.0126**	Down-Up	Down-Up	*0.00081*
1455136_at	BQ175915	*Atp1a2*	*1q21*	ATPase, Na+/K+ transporting, alpha 2	-0.578	-0.540	**-0.5588**	**0.0472**	0.338	0.323	**0.3305**	**0.0490**	Down-Up	Down-Up	*0.01636*

Table 1B. Common TG-KO changes in same direction

					DE9 TRANSGENIC				CONDITIONAL KNOCKOUT				COMPARISON		
Probe	Identifier	Symbol	Chr	Name	HC	FC	ALR TG	TG p<	HC	FC	ALR KO	KO p<	HC: TG-KO	FC: TG-KO	Overall p<
1452705_at	AK004611	*n/a*	*n/a*	Pyridoxal-dep. decarboxylase family	1.365	1.106	**1.2356**	**0.0030**	0.311	0.481	**0.3958**	**0.0465**	Up-Up	Up-Up	*0.00138*
1451447_at	BC024476	*n/a*	*n/a*	RIKEN cDNA C330016O16 gene	0.672	0.469	**0.5704**	**0.0037**	0.228	0.287	**0.2575**	**0.0057**	Up-Up	Up-Up	*0.00025*
1415694_at	AK004541	*Wars*	*14q32.31*	tryptophanyl-tRNA synthetase	0.550	0.559	**0.5544**	**0.0070**	0.253	0.379	**0.3160**	**0.0485**	Up-Up	Up-Up	*0.00307*
1419665_a_at	NM_019738	*Nupr1*	*16p11.2*	nuclear protein 1 (p8 protein)	0.404	0.238	**0.3214**	**0.0006**	0.321	0.163	**0.2417**	**0.0082**	Up-Up	Up-Up	*0.00006*
1450154_at	NM_016770	*Folh1*	*11p11.2*	folate hydrolase	-0.325	-0.109	**-0.2172**	**0.0311**	-0.290	-0.286	**-0.2878**	**0.0141**	Down-Down	Down-Down	*0.00381*
1436547_at	AV274554	*Dgke*	*17q22*	diacylglycerol kinase, epsilon	-0.361	-0.138	**-0.2493**	**0.0365**	-0.233	-0.247	**-0.2401**	**0.0063**	Down-Down	Down-Down	*0.00216*
1439241_x_at	BB825787	*n/a*	*n/a*	steroid 5 alpha-reductase 2-like	-0.398	-0.496	**-0.4470**	**0.0006**	-0.180	-0.244	**-0.2120**	**0.0172**	Down-Down	Down-Down	*0.00014*

Probe, Affymetrix probeset; Identifier, National Center for Biotechnology Information accession number; Chr, chromosomal position of gene sequence; $p <$, Student's t test probability; Overall $p <$, overall p value calculated by χ distribution.

animals used in this study have been described previously. Briefly, ΔE9 *hPS1* mice and mice carrying the human wild-type (wt) *PS1* express similar levels of *PS1* transcripts, and the encoded proteins accumulate to levels observed in nontransgenic mice (Borchelt et al., 1997; Lee et al., 1997; Lazarov et al., 2002) but result in enhanced production of Aβ_{42} peptides. Both cDNAs are driven by the mouse prion protein promoter and are expressed in a ubiquitous manner across the mouse brain. However, both the human wild-type and mutant *PS1* polypeptides fully replace the mouse *PS1* polypeptides by competing for limiting stabilization factors (Thinakaran et al., 1996; Lee et al., 1997). The ΔE9 *hPS1* mice show increased production of Aβ_{42} peptides but do not develop FAD microscopic pathology.

Mice coexpressing FAD mutant human *PS1*-ΔE9 and a chimeric mouse–human APP$_{695}$ harboring a human Aβ domain and mutations (K595N, M596L) linked to Swedish FAD pedigrees (APP$_{swe}$) have been described previously (Borchelt et al., 1997). Hippocampi of eight mice were analyzed on the same microarray platform as part of an independent environmental enrichment study. We established previously that the expression of the mutant *PS1* transgene-encoded polypeptide, ΔE9, in the APP-overexpressing mice is identical to the levels seen in mice that express *PS1*ΔE9 alone (data not shown).

Conditional *PS1* ablation in the forebrain is achieved via cre-lox recombination under calmodulin kinase 2 control (Feng et al., 2001). We have shown previously by *in situ* hybridization that *PS1* mRNA expression is no longer present in the forebrain of 10-month-old animals, and we subsequently established that forebrain ablation of *PS1* expression occurs at 6 months of age. Furthermore, in a parallel study of conditional knock-out (cKO) WT mouse *PS1* (*mPS1*), using the same CamK11cre transgene to conditionally ablate *PS1*, Yu et al. (2001) demonstrated that *PS1* protein expression is reduced by >90–95% at 6 months of age. The remaining levels of *PS1* most likely represent *PS1* expression in glial cells and vascular-associated cell types and is expected, because the conditional ablation occurs in a neuron-specific manner. Furthermore, the same study reported that *PS2* expression is not altered as a consequence of ablating *PS1* expression, whereas the levels of Aβ_{40} and Aβ_{42} were reduced by ~73 and ~25%, respectively. Unlike *PS1*/*PS2*-deficient mice (Saura et al., 2004), our mice with a conditional ablation of *PS1* are viable and do not show alterations in postenrichment contextual memory.

Sample preparation and hybridization

Hippocampi and frontal cortices were rapidly dissected, frozen on dry ice, and stored at −80°C until RNA isolation. Total RNA was isolated using the Trizol reagent. RNA quality was assessed using the Agilent Technologies (Palo Alto, CA) Bioanalyzer. Reverse transcription (RT), *in vitro* transcription, and fragmentation were performed according to the recommendation of the manufacturer. Samples were hybridized onto MOE430A mouse Affymetrix (Santa Clara, CA) GeneChips, which contained >22,000 probe sets, using the Affymetrix hybridization station. To avoid microarray batch variation, only microarrays from a single lot were used. Microarrays were considered for use only if the average 3′:5′ ratio for glyceraldehyde-3-phosphate dehydrogenase (GAPDH) and actin did not exceed 1:1.2. Of the 40 samples, three failed to meet these criteria. These were excluded from additional analyses and are denoted by the gray outline in the experimental design (see Fig. 1). Segmentation of scanned microarray images was performed by Microarray Analysis Suite 5.0. (Affymetrix). Determination of expression levels and scaling were performed using robust multichip average (Irizarry et al., 2003a,b).

Data analysis

Identification of differentially expressed genes. We identified genes as differentially expressed in the wt *hPS1*-ΔE9*hPS1* and wt *mPS1*-cKO *mPS1* comparisons if they, first, reported >0.2 average log ratio in both the hippocampal cortex (HC) and FC comparisons and, second, if the p value for both the FC and HC comparisons was <0.05. These combined criteria further increased the reliability of the data by elimination of significant, but very small, expression changes that may have a marginal biological effect (Mirnics and Pevsner, 2004).

Calculation of pooled significance. Because the expression levels are different between brain regions, the outcomes of the comparisons have to be compared independently. For calculating the combined significance between the transgenic (TG) and cKO comparisons (Table 1), the χ distribution was calculated as follows: −2*[ln(p value for TG comparison) + ln(p value for cKO comparison)]. The calculation was performed with four degrees of freedom.

Correlations. Correlations were calculated using Pearson's r value for the log$_2$ ratios between the two compared conditions.

False discovery ratio estimate. False discovery ratio (FDR) was assessed in a permutation test, in which equal numbers of experimental and con-

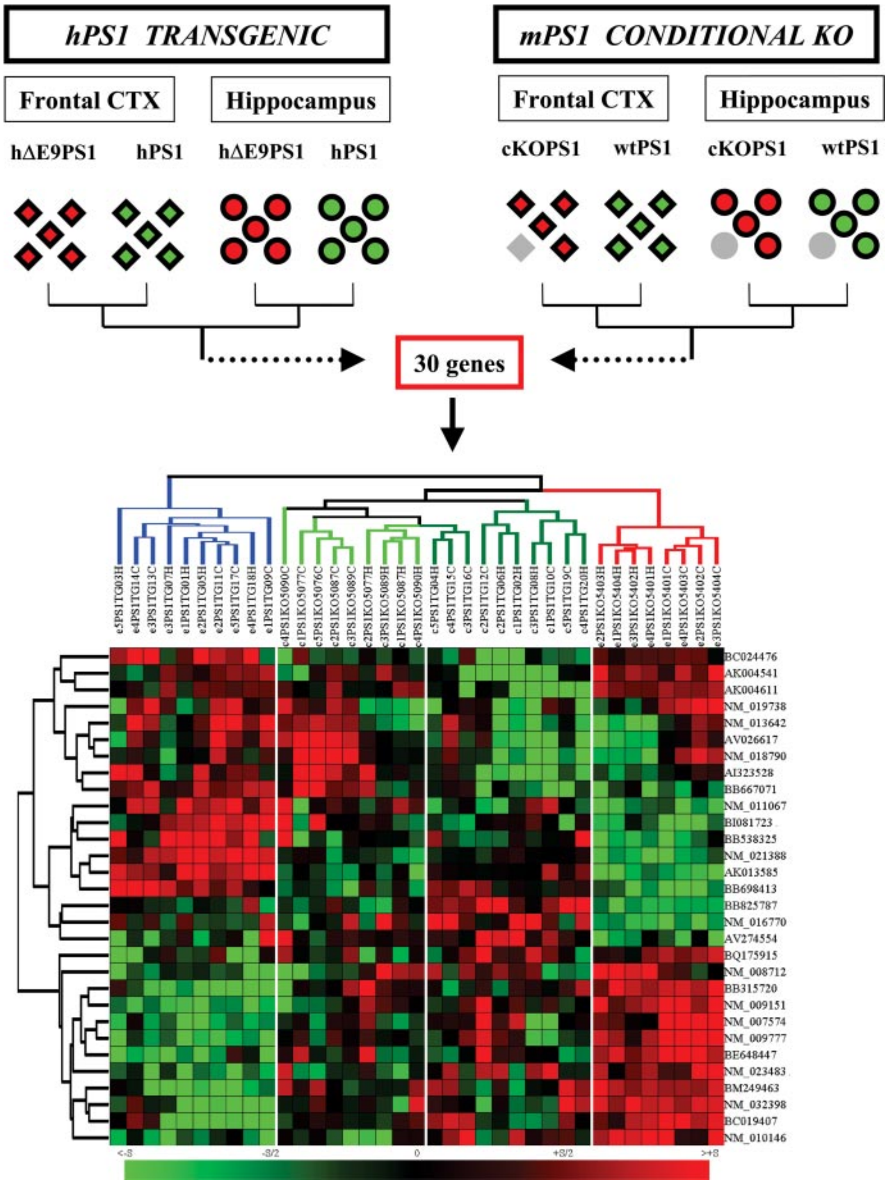

Figure 1. Experimental summary. Top, The experimental series was performed using 40 MOE430A GeneChip oligonucleotide arrays with >22,000 gene probe sets. ΔE9 *hPS1* transgenic animals were compared with mice carrying the human wild-type *PS1* gene, and conditional knock-out mice were compared with mice that did not undergo cre-lox recombination. The analysis was performed on hippocampus and frontal cortex tissue. Thirty genes were identified as differentially expressed across the HC and FC of both ΔE9 *hPS1*–wt *hPS1* and cKO *mPS1*–wt *mPS1* comparisons. Bottom, Two-way clustering of the normalized expression levels for these 30 genes separated the mouse genotypes according to their expression phenotype. In the vertical dendrogram, each arm represents a single animal (red, cKO; blue, ΔE9 *hPS1*; light green, wild-type mouse *PS1*; dark green, wild-type *hPS1*), and rows denote gene probe sets with National Center for Biotechnology Information accession numbers. Note that the cKO mice and ΔE9 mice show the largest Euclidian distance, whereas the wt *mPS1* and wt *hPS1* animals cluster adjacently. For gene names and statistical parameters, see Table 1.

trol microarrays were randomly assigned to two groups (supplemental material 1, available at www.jneurosci.org). These groups were assessed for gene expression differences with the same analysis as in the experimental–control comparison. FDR was established for each of the five permutations performed, and the mean FDR was calculated by averaging the FDR obtained in each of the permutation tests.

Clustering. Two-way clustering (sample and gene vectors) was performed on RMA-generated $\log_2$-transformed expression levels using Euclidian distance measurement in Genes@Work developed by IBM (IBM Corporation, White Plains, NY) (Lepre et al., 2004).

Custom database. RMA normalized data and statistical measurements were imported into Microsoft Access (Microsoft, Seattle, WA). This database is searchable by significance, accession number, log ratio, and gene name. The database displays individual RMA normalized data points across all experimental conditions.

Data sharing. The Microsoft Access database with all data points (~130 MB) is available on request. All of the raw microarray data have been deposited into a Gene Expression Omnibus (Edgar et al., 2002; Wheeler et al., 2004) in a Minimum Information about a Microarray Experiment/Microarray Gene Expression Data Society (Brazma et al., 2001; Ball et al., 2002; Causton and Game, 2003) compliant format and are publicly available without any restrictions.

In situ *hybridization*

In situ hybridization was performed by methods described previously (Mirnics et al., 2001b). Briefly, after designing gene-specific primers, 600–900 bp amplicons were obtained in a standard PCR. The resulting products were cloned into a vector by T/A cloning. All clones were verified by sequencing. ^{35}S-labeled antisense riboprobes were generated using T7-SP6 *in vitro* transcription and were cleaned and hybridized overnight to the tissue sections (2,000,000 dpm/slide). After washing, slides were exposed to x-ray film for up to 3 d and subsequently dipped in photoemulsion. Dipped slides were developed after 3–14 d, depending on the strength of the radioactive signal observed in film exposures. In all experiments, sense riboprobe was used as a specificity control.

Real-time quantitative PCR

For selected genes, quantitative PCR (qPCR) was performed on pooled samples from the five groups of animals (wt *hPS1*, ΔE9 *hPS1*, wt *mPS1*, cKO *mPS1*, and ΔE9 *hPS1* × APP_{695}). After primer validation for amplification efficiency (95–100%), the experiment was performed using standard Δ Ct-Sybr Green measurement protocols with two independent reverse transcriptions and four replicates per RT (Mimmack et al., 2004). GAPDH was used as a standard normalizer. Primer sequences are available in supplemental material 2 (available at www.jneurosci.org).

Results

RNA was harvested from HCs and FCs from five CKO *mPS1* and five control wt *mPS1* animals. Conditional ablation is achieved by cre-lox recombination under calmodulin kinase 2 control previously generated in our laboratory (Fig. 1, top right). These cKO mice are viable and do not develop any obvious pathology with aging. Each sample was hybridized to a single MOE430AGeneChip (20 arrays in total). The obtained intensity measurements were normalized by RMA (Irizarry et al., 2003a,b) and imported into a custom-made Microsoft Access database. Because we were interested in the overall influence of the *PS1* ablation on the transcriptome of two AD-affected brain regions, we focused our attention to expression changes that were present in both HC and FC. This analysis identified 85 genes that were differentially expressed across both regions (Fig. 1) (supplemental material 3, available at www.jneurosci.org) and will be referred to as the "KO comparison." For these 85 genes, the correlation between the outcome of the HC and FC comparisons was $r = 0.96$ ($p < 0.0001$). The number of genes with increased and decreased expression was evenly distributed, with transcript reductions showing a greater magnitude than transcript inductions.

Once we defined a *PS1*-dependent transcript network, we were interested to determine whether the expression profiles of the cKO animal share any commonalities with that of humanized mice carrying the ΔE9 *hPS1* mutation. As a result, we chose to perform a microarray analysis on the HC and FC of the ΔE9 *hPS1* mutants using a similar experimental design used in the cKO experiment. We hypothesized that the most critical expression changes produced the conditional ablation of *PS1* might also appear in the ΔE9 *hPS1* variant. We speculated that if the mutant human *PS1* polypeptide was a hypermorph, or "gain of function" species, differences in ΔE9 *hPS1* mice would be in the opposite direction than in the *PS1* cKO animals. However, if both the ΔE9 *hPS1* and cKO *PS1* animals show expression changes in the same direction, this would suggest that these changes are related to the "loss of function" effect of the human mutant *PS1*. When compared with the wt *hPS1* transgenic animal (also referred to as a "TG comparison"), ΔE9 *hPS1* mice reported 71 gene expression changes (supplemental material 4, available at www.jneurosci.org). The expression ratios of these 71 genes identified as differentially expressed were highly correlated between the HC and FC comparisons ($r = 0.97$; $p < 0.0001$). Twenty-two genes were downregulated, whereas 49 genes were upregulated in these animals. Contrary to the cKO comparison, the ΔE9 *hPS1* mice showed more robust transcript upregulations than mRNA level reductions. Selected expression changes were verified for several genes on two additional pairs of transgenic animals using *in situ* hybridization (Fig. 2). In these experiments, maternally expressed gene 3 (MEG3), exostoses-like 2 (EXL2), hippocampus-abundant transcript 1 (HIAT1), activity-related cytoskeletal protein (ARC), and amylase 1A (AMY1A) all validated the microarray-predicted expression changes between the two sets of transgenic animals.

When the two datasets were cross-compared, 30 genes showed a robust and significant change in both TG and cKO comparisons. When the normalized adjusted intensities for the whole dataset were two-way clustered for the commonly changed 30 genes, the four experimental groups (wt *mPS1*, *hPS1*, ΔE9 *hPS1*, and cKO *mPS1*) separated into distinct clusters (Fig. 1, bottom). The ΔE9 *hPS1* and the cKO *mPS1* mice showed the greatest Euclidian distance, with the two control groups (*hPS1* and *mPS1*) clustering in between. For the group of 30 genes, there was a high correlation in the expression ratio between the HC and FC across the two conditions and within the ΔE9 and cKO mice (Fig. 3). FDR assessment by permutation of the dataset suggested that by random chance, less than one gene would show the observed gene expression changes (<2% of the observed changes) (supplemental material 1, available at www.jneurosci.org)

Of the 30 genes, 23 genes were regulated in the opposite direction (up–down or down–up), whereas seven showed expression changes that were similar in direction (Table 1). For all genes, HC and FC data reported a consistent change of direction. Of the 23 transcripts that were regulated in an opposite direction in the TG and cKO mice comparisons, 11 genes reported increases in the ΔE9 *hPS1* mice and decreases in the cKO *mPS1* mice, and 12 genes reported a decrease in the ΔE9 *hPS1* mice and increases in the cKO *mPS1* mice. Of the seven genes that were changed in the

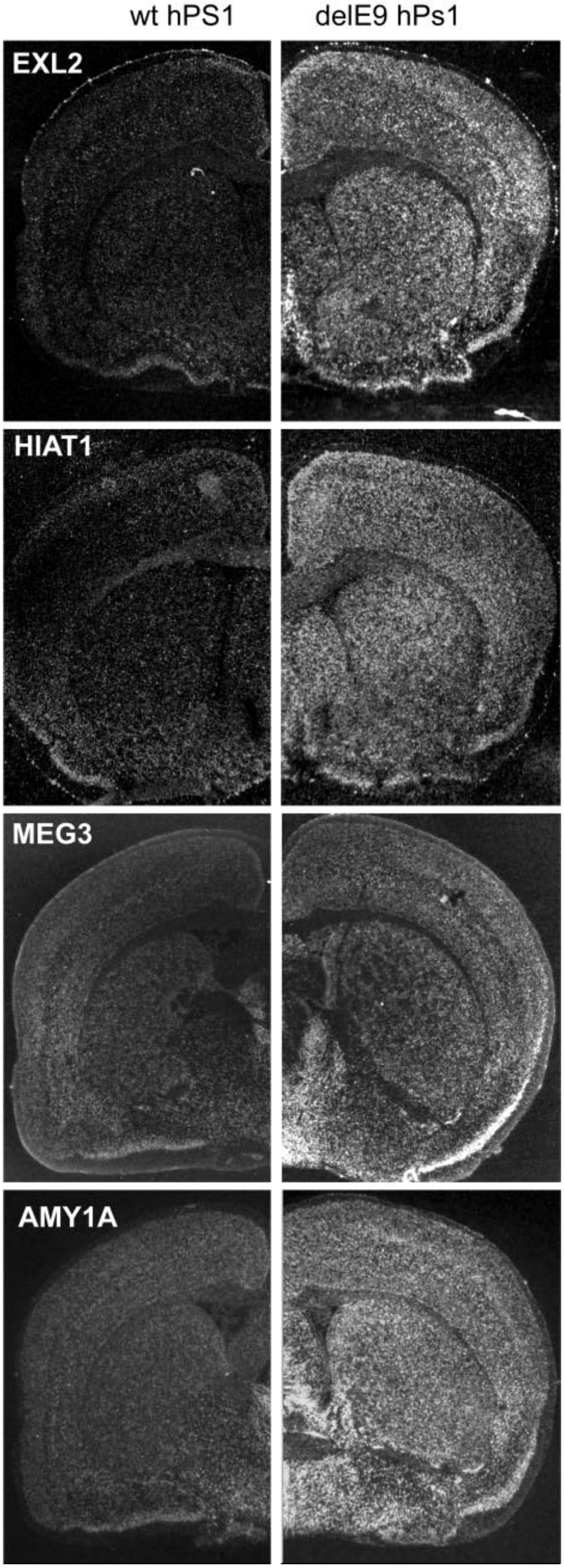

Figure 2. Verification of TG comparison data by *in situ* hybridization. Low-magnification, dark-field composite micrographs of ΔE9 *hPS1* (right column) and wt *hPS1* (left column) mice brain sections. Riboprobes for EXL2, HIAT1, MEG3, and AMY1A were hybridized to 20-μm-thick coronal sections using methods described previously. For the investigated genes, the *in situ* hybridization data were in concordance with the microarray findings.

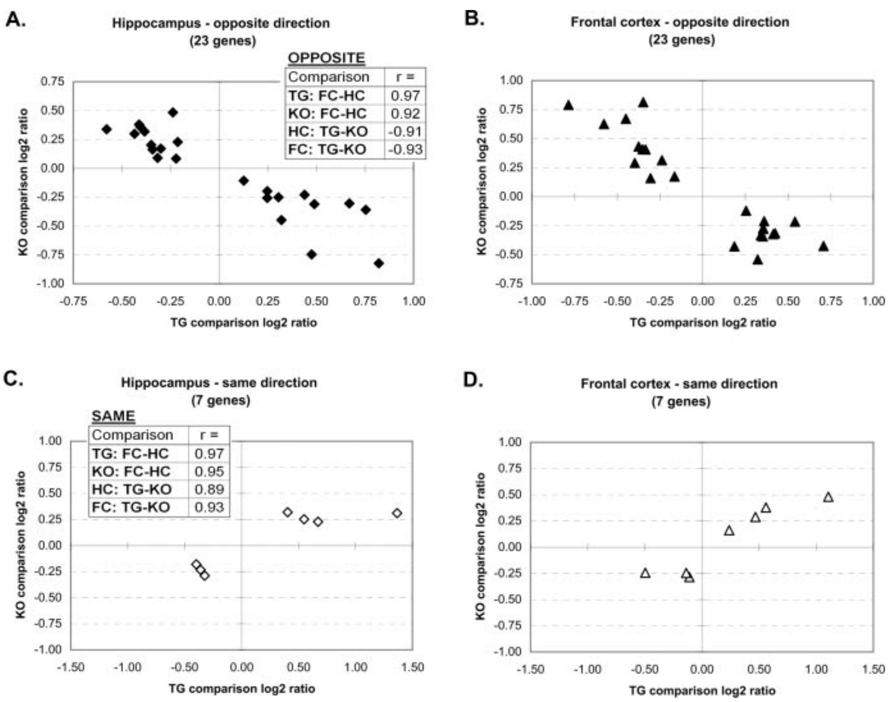

Figure 3. Coregulation of genes across the TG and cKO comparisons. *A*, *B*, Expression changes in the hippocampus (*A*) and frontal cortex (*B*) for the 23 genes changed in the opposite direction. The *x*-axis represents TG comparison $\log_2$ ratio, and the *y*-axis denotes cKO comparison $\log_2$ ratio. *C*, *D*, Expression changes of seven genes that were regulated in a similar direction in both the TG and cKO comparisons. Graph layout is similar to that in *A* and *B*. Inserted tables in *A* and *C* denote statistical correlations across the TG and cKO comparisons and across the two brain regions (HC and FC). Note the high degree of transcript coregulation across both the TG and cKO comparisons and HC and FC.

same direction in both the ΔE9 and cKO mice, four genes reported transcript induction and three genes reported transcript repression. In addition to the 30 genes that showed unequivocal regulation in both systems, we identified an additional 72 genes that showed some evidence for regulation in both the ΔE9 and cKO comparisons (supplemental material 5, available at www.jneurosci.org). Although these gene probes satisfied only three of four statistical criteria we used in the current study [average $\log_2$ ratio (ALR) >0.20 and $p < 0.05$ in both TG and cKO comparisons], this group very likely contains biologically meaningful data, because of the following: (1) the majority of the probes in this group still reported an overall significance across the combined dataset; (2) eight genes were represented with multiple, independent probe sets that showed consistent findings; (3) 63 of the 72 probes showed consistent results between the HC and FC comparison; (4) two-way clustering of the 102 putatively changed genes resulted in an outstanding separation of the ΔE9 *hPS1* and cKO *mPS1* experimental groups (supplemental material 6, available at www.jneurosci.org); and (5) FDR assessment suggested that ~80% of the observed gene expression changes can be attributed to real data discovery (supplemental material 1, available at www.jneurosci.org).

Although the expression of ΔE9 *hPS1* leads to elevated $A\beta_{42}$ production, the overall level of Aβ production is extremely low in the brains of nontransgenic mice. As a result, we felt it was critical to investigate ΔE9 *hPS1*-driven expression changes in the context of high-APP levels. To achieve this, we compared the expression in the hippocampus of five ΔE9 *hPS1* mutant mice to that of eight ΔE9 *hPS1* × APP_{695} Swe mice generated in our previous study (Lazarov et al., 2002). Surprisingly, the commonly regulated 30 genes that were the most strongly regulated in both the TG and cKO comparisons (Table 1) showed a strong inverse correlation ($r = -0.72$; $p < 0.001$) in the ΔE9 *hPS1* × APP_{695} Swe versus ΔE9 *hPS1* comparison: 25 of the 30 genes examined showed an expression change that was opposite in direction than observed in the ΔE9 *hPS1* versus wt *hPS1* comparison (Fig. 4).

Finally, for seven of the 30 genes across the five different groups of mice (wt *hPS1*, ΔE9 *hPS1*, wt *mPS1*, cKO *mPS1*, and ΔE9 *hPS1* × APP_{695} Swe), we decided to confirm the expression changes by real-time qPCR in the hippocampus (Fig. 5). In the qPCR assessment, Fos, DUSP1 (MAP kinase phosphatase-1, serine/threonine-specific protein phosphatase), ARC, EXL2, cyclin D1, C1Qb, and C1Qg expression levels were changed in the microarray-predicted direction. The microarray-reported expression changes (ALR) were highly correlated ($r = 0.91$; $p < 0.001$), with the qPCR reported expression changes (ΔΔCt) across the five different sample groups. The expression changes were more robust in the qPCR data than the GeneChip findings, suggesting that the microarray dataset may underestimate the actual expression differences.

Discussion

In this study, we identified the transcriptome profile of ΔE9 *hPS1*, wt *hPS1*, cKO *mPS1*, and wt *mPS1* mice. Transcriptome responses observed in both the TG and cKO comparisons were highly correlated between the HC and FC. Thirty genes that were changed in the ΔE9 *hPS1*–wt *hPS1* comparison also showed an expression change in the *mPS1*-ablated and wild-type mice comparison, suggesting that these expression changes represent the critical effect of the ΔE9 *hPS1* variant on the transcriptome. In the second part of this study, the comparison of ΔE9 *hPS1* with the ΔE9 *hPS1* × APP_{695} Swe mice revealed that the combined expression of ΔE9 *hPS1* and APP_{695} Swe has a very strong influence on the expression of the same 30 genes identified in the TG and cKO comparisons: 25 of the 30 genes reported transcript level changes that were opposite in direction to those observed in the ΔE9 *hPS1* single mutants.

The effect of *PS1* mutation on the transcriptome: gain of function or loss of function?

FAD-linked *PS1* variants have been primarily considered to lead to a gain of function. However, recent data suggest that these FAD-linked *PS1* variants, in addition to gain of function effects, may also lead to loss of function properties (Cai et al., 2003; De Strooper and Woodgett, 2003; Marjaux et al., 2004; Saura et al., 2004). Our dataset is very informative in this regard: 23 of 30 genes (and 72 of 102 genes in the extended dataset) showed expression alterations that were opposite in direction between the TG and cKO comparisons. These data strongly support the view that, at least at the transcriptome level, the expression changes associated with the ΔE9 *hPS1* mutation are a result of a gain of function. However, it should be noted that the ΔE9 *hPS1* expression did not result only in transcript increases. Rather, expression increases and decreases were evenly distributed (11 upregulations and 12 downregulations), suggesting that transcript downregulations may be an equally important consequence of the ΔE9 *hPS1* mutation as the upregulations; the obtained data argues that the mutant ΔE9 *hPS1* is also a potent negative regulator of transcript levels.

The minority of genes (seven transcripts) were regulated in the same direction in the TG and cKO comparisons. The finding that the ΔE9 *hPS1* mutation produces some of the same effects as seen in *PS1* ablation is not unexpected and represents a strong argument for loss of function events that may occur in conjunction with this mutation.

The critical *PS1*-dependent transcript network

The expression levels of 30 genes that we identified in both the TG and cKO comparisons strongly depend on *PS1* expression and function. Multiple genes of this group have been previously associated with AD, neurodegenerative diseases, or cognitive performance. Increased immunoreactivity for Fos-related proteins in Alzheimer's disease has been observed in multiple studies (Zhang et al., 1992; Anderson et al., 1994; Marcus et al., 1998), and activation of c-Fos contributes to amyloid β-peptide-induced neurotoxicity (Gillardon et al., 1996). In addition to Fos and Arc, several other genes we found have been implicated in the pathophysiology of AD and/or cognitive processes. For example, strong upregulation of Gadd45, indicating DNA damage, is an early event in Aβ cytotoxicity (Santiard-Baron et al., 1999). Furthermore, the presence of neuronal nitric oxide synthase (NOS) in pyramidal-like neurons is a distinct characteristic of AD (Fernandez-Vizarra et al., 2004), and familial *PS1* mutations in the N-terminal fragment cause NOS inhibitor-sensitive neuronal cell death (Hashimoto et al., 2004). In addition, C1q has been postulated to play a significant role in AD pathogenesis by multiple studies (Matsuoka et al., 2001; Luo et al., 2003; Veerhuis et al., 2003; Fonseca et al., 2004). In a transgenic animal model, Matsuoka et al. (2001) found that C1q levels increase as a result of fibrillar Aβ production, whereas Veerhuis et al. (2003) argue that C1q-containing Aβ deposits precede, or occur commensurate with, neurodegenerative changes in AD. Furthermore, Luo et al. (2003) suggest that the C1q may mediate neuronal injury during AD by contributing to neuronal oxidative stress and neuronal demise. Finally, it is known that Tau protein and, in some cases, neurofilament subunits exhibit abnormal phosphorylation on specific serine and threonine residues in AD and frontotemporal dementia (for review, see Morfini et al., 2002), and this may be directly related to the expression changes in DUSP1 we observed.

Recent studies of Dickey et al. (2003, 2004) are highly relevant for the interpretation of our dataset. Although these studies and our present dataset were generated with very different experimental parameters (age of mice, pooling, replicates, strain of

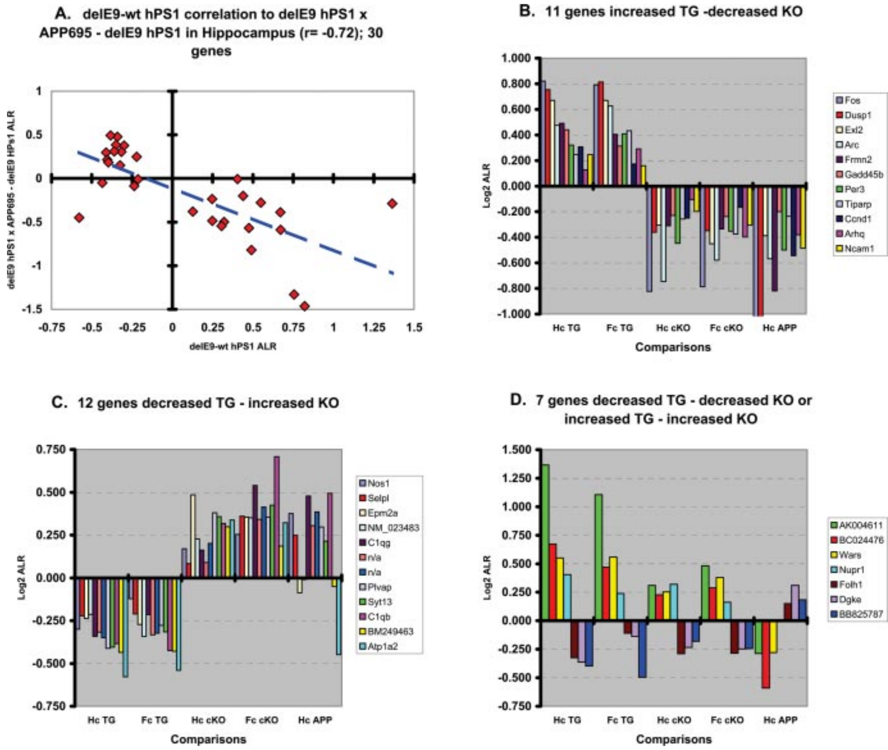

Figure 4. Coregulation of gene expression between the ΔE9 *hPS1* × APP_{695} double-transgenic and ΔE9 *hPS1* single-transgenic animals. *A*, The 30 genes identified in the TG and cKO comparisons also showed robust transcription changes in the ΔE9 *hPS1* × APP_{695} mice. The *x*-axis represents TG comparison $\log_2$ ratio (ΔE9 *hPS1* vs wt *hPS1*), and the *y*-axis denotes ΔE9 *hPS1* × APP_{695} versus ΔE9 *hPS1* comparison $\log_2$ ratio in the hippocampus. The blue dashed line represents the trend line. Note that the 30 genes examined show a strong and inverse coregulation ($r = -0.72$; $p < 0.001$) across the two comparisons, suggesting a robust effect of APP on the ΔE9 *hPS1* background. *B–D*, Individual gene expression changes across the ΔE9 *hPS1* × APP_{695} versus ΔE9 *hPS1* comparison. The *x*-axis represents sample class, and the *y*-axis denotes comparison $\log_2$ ratio. For gene abbreviations, see Table 1. Note that the majority of genes are regulated in different directions between the TG and ΔE9 *hPS1* × APP_{695} versus ΔE9 *hPS1* comparisons.

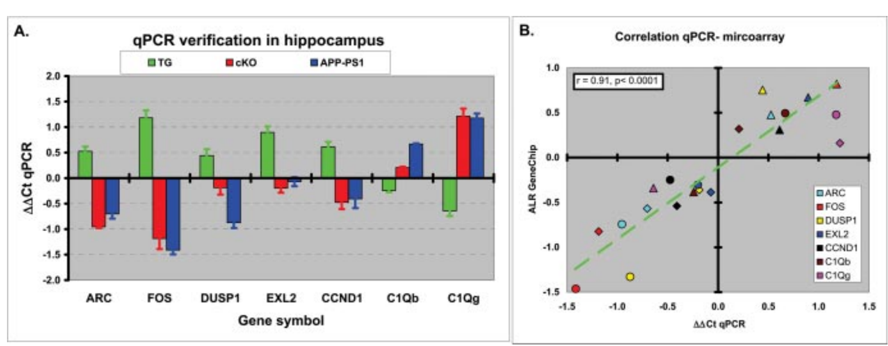

Figure 5. RT-qPCR verification of microarray data for seven genes. *A*, The *x*-axis represents genes, and the *y*-axis denotes average ΔΔCt from two independent reverse transcriptions (4 replicates each). The green bars denote TG comparison (ΔE9 *hPS1* vs wt *hPS1*), the red bars correspond to cKO comparison (cKO *mPS1* vs wt *mPS1*), and the blue bars indicate expression change in the APP–*PS1* comparison (ΔE9 *hPS1* × APP_{695} vs ΔE9 *hPS1*). Error bars denote SD. For gene symbols, see Table 1. *B*, Correlation of microarray data with qPCR data. The *x*-axis represents qPCR ΔΔCt, and the *y*-axis denotes the ALR established in the microarray comparisons. Colors denote different genes, and shapes denote comparisons (triangle, TG comparison; circle, cKO comparison; diamond, APP–*PS1* comparison). The green dashed line denotes the linear trend. Note that the data show a strong and significant correlation ($r = 0.91$; $p < 0.0001$).

mice, controls, and microarray platform used), they both report a downregulation of several genes (e.g., Arc, Egr, Fos) in the APP × *PS1* double-mutant mice. Thus, the combined data suggest that the expression changes in at least some of the genes we observed is a persistent hallmark of the disease model. These changes appear to be present both before the pathology develops (3 months; our present dataset) and during the Aβ deposition phase (17–18 months) (Dickey et al., 2003). Furthermore, this downregulation is observed in two different lines of mutant mice [$\mathrm{APP}_{\mathrm{K670N,M671L}}$ × *PS1*–5.1 (Dickey et al., 2003) and APP_{695} Swe × ΔE9 *PS1* (our study)] and suggests that this process is directly related to the pathophysiological processes associated with the expression of mutant APP and *PS1* variants, rather than the exact experimental model.

Directionality of expression changes

Regulation of the 30 genes across the different conditions also argues that these are part of a common, strongly coregulated, transcript network that depends on normal *PS1* function. These genes indicate an intriguing expression pattern across the hippocampus of the TG, conditional KO, and ΔE9 *hPS1* × APP_{695} Swe versus ΔE9 *hPS1* comparisons, suggesting that they may be critically involved in pathophysiological changes that lead to experimental AD and perhaps human pathology. In this context, we interpret that the majority of expression changes in the TG comparison are the result of gain of function effects of the ΔE9 *hPS1*. However, because the level of endogenously generated $A\beta_{42}$ in mouse brain is extremely low (Duff et al., 1996), the small increase in the levels of $A\beta_{42}$ after expression of mutant *PS1* may be stimulatory rather than toxic. Nevertheless, it is important to point out that in our system, the mutant *PS1*-dependent expression changes clearly depend on APP/Aβ levels. Once the same mutant *PS1* is coexpressed with APP (in the ΔE9 *hPS1* × APP_{695} Swe mice), the levels of APP, as well as the neurotoxic $A\beta_{42}$ peptide, are markedly elevated, leading to expression changes that are opposite those observed in the ΔE9 *hPS1* single-mutant mice. Based on our results, we argue that the physiological effects of expressing *PS1* mutants have two essential components: one that is constant and is a direct result of the mutation, and a second that depends on APP and $A\beta_{42}$ levels.

At present, the role of those genes that are subject to *PS1*-dependant regulation are not established, but we suggest that for at least a subset of these genes, the levels of expression may be critical for cognitive performance. For example, disruption of Arc, Fos, or Egr-1 expression, either by intrahippocampal administration of antisense oligonucleotides or by germline disruption, impairs consolidation of long-term memory formation (Guzowski, 2002; Steward and Worley, 2002; Vazdarjanova et al., 2002; Montag-Sallaz and Montag, 2003). Furthermore, elegant microarray studies on aging by Blalock et al. (2004) have also identified Arc and NR4A as important aging- and cognition-related genes. Thus, we speculate that the observed gene expression changes may be directly relevant for the pathophysiology of aging, cognition, and/or Alzheimer's disease.

References

Anderson AJ, Cummings BJ, Cotman CW (1994) Increased immunoreactivity for Jun- and Fos-related proteins in Alzheimer's disease: association with pathology. Exp Neurol 125:286–295.

Ball CA, Sherlock G, Parkinson H, Rocca-Sera P, Brooksbank C, Causton HC, Cavalieri D, Gaasterland T, Hingamp P, Holstege F, Ringwald M, Spellman P, Stoeckert Jr CJ, Stewart JE, Taylor R, Brazma A, Quackenbush J (2002) Standards for microarray data. Science 298:539.

Blalock EM, Geddes JW, Chen KC, Porter NM, Markesbery WR, Landfield PW (2004) Incipient Alzheimer's disease: microarray correlation analyses reveal major transcriptional and tumor suppressor responses. Proc Natl Acad Sci USA 101:2173–2178.

Borchelt DR, Thinakaran G, Eckman CB, Lee MK, Davenport F, Ratovitsky T, Prada CM, Kim G, Seekins S, Yager D, Slunt HH, Wang R, Seeger M, Levey AI, Gandy SE, Copeland NG, Jenkins NA, Price DL, Younkin SG, Sisodia SS (1996) Familial Alzheimer's disease-linked presenilin 1 variants elevate Abeta1–42/1–40 ratio *in vitro* and *in vivo*. Neuron 17:1005–1013.

Borchelt DR, Ratovitski T, van Lare J, Lee MK, Gonzales V, Jenkins NA, Copeland NG, Price DL, Sisodia SS (1997) Accelerated amyloid deposition in the brains of transgenic mice coexpressing mutant presenilin 1 and amyloid precursor proteins. Neuron 19:939–945.

Brazma A, Hingamp P, Quackenbush J, Sherlock G, Spellman P, Stoeckert C, Aach J, Ansorge W, Ball CA, Causton HC, Gaasterland T, Glenisson P, Holstege FC, Kim IF, Markowitz V, Matese JC, Parkinson H, Robinson A, Sarkans U, Schulze-Kremer S, et al. (2001) Minimum information about a microarray experiment (MIAME)-toward standards for microarray data. Nat Genet 29:365–371.

Cai D, Leem JY, Greenfield JP, Wang P, Kim BS, Wang R, Lopes KO, Kim SH, Zheng H, Greengard P, Sisodia SS, Thinakaran G, Xu H (2003) Presenilin-1 regulates intracellular trafficking and cell surface delivery of beta-amyloid precursor protein. J Biol Chem 278:3446–3454.

Causton HC, Game L (2003) MGED comes of age. Genome Biol 4:351.

Colangelo V, Schurr J, Ball MJ, Pelaez RP, Bazan NG, Lukiw WJ (2002) Gene expression profiling of 12633 genes in Alzheimer hippocampal CA1: transcription and neurotrophic factor down-regulation and up-regulation of apoptotic and pro-inflammatory signaling. J Neurosci Res 70:462–473.

De Strooper B (2003) Aph-1, Pen-2, and nicastrin with presenilin generate an active gamma-secretase complex. Neuron 38:9–12.

De Strooper B, Woodgett J (2003) Alzheimer's disease: mental plaque removal. Nature 423:392–393.

Dickey CA, Loring JF, Montgomery J, Gordon MN, Eastman PS, Morgan D (2003) Selectively reduced expression of synaptic plasticity-related genes in amyloid precursor protein + presenilin-1 transgenic mice. J Neurosci 23:5219–5226.

Dickey CA, Gordon MN, Mason JE, Wilson NJ, Diamond DM, Guzowski JF, Morgan D (2004) Amyloid suppresses induction of genes critical for memory consolidation in APP + *PS1* transgenic mice. J Neurochem 88:434–442.

Duff K, Eckman C, Zehr C, Yu X, Prada CM, Perez-tur J, Hutton M, Buee L, Harigaya Y, Yager D, Morgan D, Gordon MN, Holcomb L, Refolo L, Zenk B, Hardy J, Younkin S (1996) Increased amyloid-beta42(43) in brains of mice expressing mutant presenilin 1. Nature 383:710–713.

Edgar R, Domrachev M, Lash AE (2002) Gene expression omnibus: NCBI gene expression and hybridization array data repository. Nucleic Acids Res 30:207–210.

Feng R, Rampon C, Tang YP, Shrom D, Jin J, Kyin M, Sopher B, Miller MW, Ware CB, Martin GM, Kim SH, Langdon RB, Sisodia SS, Tsien JZ (2001) Deficient neurogenesis in forebrain-specific presenilin-1 knockout mice is associated with reduced clearance of hippocampal memory traces. Neuron 32:911–926.

Fernandez-Vizarra P, Fernandez AP, Castro-Blanco S, Encinas JM, Serrano J, Bentura ML, Munoz P, Martinez-Murillo R, Rodrigo J (2004) Expression of nitric oxide system in clinically evaluated cases of Alzheimer's disease. Neurobiol Dis 15:287–305.

Fonseca MI, Kawas CH, Troncoso JC, Tenner AJ (2004) Neuronal localization of C1q in preclinical Alzheimer's disease. Neurobiol Dis 15:40–46.

Gan L, Ye S, Chu A, Anton K, Yi S, Vincent VA, von Schack D, Chin D, Murray J, Lohr S, Patthy L, Gonzalez-Zulueta M, Nikolich K, Urfer R (2004) Identification of cathepsin B as a mediator of neuronal death induced by Aβ-activated microglial cells using a functional genomics approach. J Biol Chem 279:5565–5572.

Gillardon F, Skutella T, Uhlmann E, Holsboer F, Zimmermann M, Behl C (1996) Activation of c-Fos contributes to amyloid beta-peptide-induced neurotoxicity. Brain Res 706:169–172.

Ginsberg SD, Hemby SE, Lee VM, Eberwine JH, Trojanowski JQ (2000) Expression profile of transcripts in Alzheimer's disease tangle-bearing CA1 neurons. Ann Neurol 48:77–87.

Guzowski JF (2002) Insights into immediate-early gene function in hippocampal memory consolidation using antisense oligonucleotide and fluorescent imaging approaches. Hippocampus 12:86–104.

Hashimoto Y, Tsukamoto E, Niikura T, Yamagishi Y, Ishizaka M, Aiso S, Takashima A, Nishimoto I (2004) Amino- and carboxyl-terminal mutants of presenilin 1 cause neuronal cell death through distinct toxic mechanisms: study of 27 different presenilin 1 mutants. J Neurosci Res 75:417–428.

Ho L, Guo Y, Spielman L, Petrescu O, Haroutunian V, Purohit D, Czernik A, Yemul S, Aisen PS, Mohs R, Pasinetti GM (2001) Altered expression of a-type but not b-type synapsin isoform in the brain of patients at high risk for Alzheimer's disease assessed by DNA microarray technique. Neurosci Lett 298:191–194.

Irizarry RA, Bolstad BM, Collin F, Cope LM, Hobbs B, Speed TP (2003a) Summaries of Affymetrix GeneChip probe level data. Nucleic Acids Res 31:e15.

Irizarry RA, Hobbs B, Collin F, Beazer-Barclay YD, Antonellis KJ, Scherf U, Speed TP (2003b) Exploration, normalization, and summaries of high density oligonucleotide array probe level data. Biostatistics 4:249–264.

Lazarov O, Lee M, Peterson DA, Sisodia SS (2002) Evidence that synaptically released β-amyloid accumulates as extracellular deposits in the hippocampus of transgenic mice. J Neurosci 22:9785–9793.

Lee MK, Borchelt DR, Kim G, Thinakaran G, Slunt HH, Ratovitski T, Martin LJ, Kittur A, Gandy S, Levey AI, Jenkins N, Copeland N, Price DL, Sisodia SS (1997) Hyperaccumulation of FAD-linked presenilin 1 variants *in vivo*. Nat Med 3:756–760.

Lepre J, Rice JJ, Tu Y, Stolovitzky G (2004) Genes@Work: an efficient algorithm for pattern discovery and multivariate feature selection in gene expression data. Bioinformatics 20:1033–1044.

Loring JF, Wen X, Lee JM, Seilhamer J, Somogyi R (2001) A gene expression profile of Alzheimer's disease. DNA Cell Biol 20:683–695.

Luo X, Weber GA, Zheng J, Gendelman HE, Ikezu T (2003) C1q-calreticulin induced oxidative neurotoxicity: relevance for the neuropathogenesis of Alzheimer's disease. J Neuroimmunol 135:62–71.

Marcotte ER, Srivastava LK, Quirion R (2003) cDNA microarray and proteomic approaches in the study of brain diseases: focus on schizophrenia and Alzheimer's disease. Pharmacol Ther 100:63–74.

Marcus DL, Strafaci JA, Miller DC, Masia S, Thomas CG, Rosman J, Hussain S, Freedman ML (1998) Quantitative neuronal c-*fos* and c-*jun* expression in Alzheimer's disease. Neurobiol Aging 19:393–400.

Marjaux E, Hartmann D, De Strooper B (2004) Presenilins in memory, Alzheimer's disease, and therapy. Neuron 42:189–192.

Matsuoka Y, Picciano M, Malester B, LaFrancois J, Zehr C, Daeschner JM, Olschowka JA, Fonseca MI, O'Banion MK, Tenner AJ, Lemere CA, Duff K (2001) Inflammatory responses to amyloidosis in a transgenic mouse model of Alzheimer's disease. Am J Pathol 158:1345–1354.

Mimmack ML, Brooking J, Bahn S (2004) Quantitative polymerase chain reaction: validation of microarray results from postmortem brain studies. Biol Psychiatry 55:337–345.

Mirnics K, Pevsner J (2004) Progress in the use of microarray technology to study the neurobiology of disease. Nat Neurosci 7:434–439.

Mirnics K, Middleton FA, Lewis DA, Levitt P (2001a) Analysis of complex brain disorders with gene expression microarrays: schizophrenia as a disease of the synapse. Trends Neurosci 24:479–486.

Mirnics K, Middleton FA, Stanwood GD, Lewis DA, Levitt P (2001b) Disease-specific changes in regulator of G-protein signaling 4 (RGS4) expression in schizophrenia. Mol Psychiatry 6:293–301.

Mirnics ZK, Mirnics K, Terrano D, Lewis DA, Sisodia SS, Schor NF (2003) DNA microarray profiling of developing *PS1*-deficient mouse brain reveals complex and coregulated expression changes. Mol Psychiatry 8:863–878.

Montag-Sallaz M, Montag D (2003) Learning-induced arg 3.1/arc mRNA expression in the mouse brain. Learn Mem 10:99–107.

Morfini G, Pigino G, Beffert U, Busciglio J, Brady ST (2002) Fast axonal transport misregulation and Alzheimer's disease. Neuromolecular Med 2:89–99.

Mufson EJ, Counts SE, Ginsberg SD (2002) Gene expression profiles of cholinergic nucleus basalis neurons in Alzheimer's disease. Neurochem Res 27:1035–1048.

Price DL, Tanzi RE, Borchelt DR, Sisodia SS (1998) Alzheimer's disease: genetic studies and transgenic models. Annu Rev Genet 32:461–493.

Rogaev EI, Sherrington R, Rogaeva EA, Levesque G, Ikeda M, Liang Y, Chi H, Lin C, Holman K, Tsuda T, Mar L, Sorbi S, Nacmias B, Piacentini S, Amaducci L, Chumakov I, Cohen D, Lannfelt L, Fraser PE, Rommens JM, et al. (1995) Familial Alzheimer's disease in kindreds with missense mutations in a gene on chromosome 1 related to the Alzheimer's disease type 3 gene. Nature 376:775–778.

Santiard-Baron D, Gosset P, Nicole A, Sinet PM, Christen Y, Ceballos-Picot I (1999) Identification of beta-amyloid-responsive genes by RNA differential display: early induction of a DNA damage-inducible gene, gadd45. Exp Neurol 158:206–213.

Saura CA, Choi SY, Beglopoulos V, Malkani S, Zhang D, Shankaranarayana Rao BS, Chattarji S, Kelleher III RJ, Kandel ER, Duff K, Kirkwood A, Shen J (2004) Loss of presenilin function causes impairments of memory and synaptic plasticity followed by age-dependent neurodegeneration. Neuron 42:23–36.

Scheuner D, Eckman C, Jensen M, Song X, Citron M, Suzuki N, Bird TD, Hardy J, Hutton M, Kukull W, Larson E, Levy-Lahad E, Viitanen M, Peskind E, Poorkaj P, Schellenberg G, Tanzi R, Wasco W, Lannfelt L, Selkoe D, et al. (1996) Secreted amyloid beta-protein similar to that in the senile plaques of Alzheimer's disease is increased *in vivo* by the presenilin 1 and 2 and APP mutations linked to familial Alzheimer's disease. Nat Med 2:864–870.

Selkoe DJ (2001) Presenilin, Notch, and the genesis and treatment of Alzheimer's disease. Proc Natl Acad Sci USA 98:11039–11041.

Sherrington R, Rogaev EI, Liang Y, Rogaeva EA, Levesque G, Ikeda M, Chi H, Lin C, Li G, Holman K, Tsuda T, Mar L, Foncin J-F, Bruni AC, Montesi MP, Sorbi S, Rainero I, Pinessi L, Nee L, Chumakov I, et al. (1995) Cloning of a gene bearing missense mutations in early-onset familial Alzheimer's disease. Nature 375:754–760.

Steward O, Worley P (2002) Local synthesis of proteins at synaptic sites on dendrites: role in synaptic plasticity and memory consolidation? Neurobiol Learn Mem 78:508–527.

Thinakaran G, Borchelt DR, Lee MK, Slunt HH, Spitzer L, Kim G, Ratovitsky T, Davenport F, Nordstedt C, Seeger M, Hardy J, Levey AI, Gandy SE, Jenkins NA, Copeland NG, Price DL, Sisodia SS (1996) Endoproteolysis of presenilin 1 and accumulation of processed derivatives *in vivo*. Neuron 17:181–190.

Van Gassen G, Annaert W (2003) Amyloid, presenilins, and Alzheimer's disease. Neuroscientist 9:117–126.

Vazdarjanova A, McNaughton BL, Barnes CA, Worley PF, Guzowski JF (2002) Experience-dependent coincident expression of the effector immediate-early genes *arc* and *Homer 1a* in hippocampal and neocortical neuronal networks. J Neurosci 22:10067–10071.

Veerhuis R, Van Breemen MJ, Hoozemans JM, Morbin M, Ouladhadj J, Tagliavini F, Eikelenboom P (2003) Amyloid β plaque-associated proteins C1q and SAP enhance the Aβ1–42 peptide-induced cytokine secretion by adult human microglia *in vitro*. Acta Neuropathol (Berl) 105:135–144.

Wang CC, Kadota M, Nishigaki R, Kazuki Y, Shirayoshi Y, Rogers MS, Gojobori T, Ikeo K, Oshimura M (2004) Molecular hierarchy in neurons differentiated from mouse ES cells containing a single human chromosome 21. Biochem Biophys Res Commun 314:335–350.

Wheeler DL, Church DM, Edgar R, Federhen S, Helmberg W, Madden TL, Pontius JU, Schuler GD, Schriml LM, Sequeira E, Suzek TO, Tatusova TA, Wagner L (2004) Database resources of the National Center for Biotechnology Information: update. Nucleic Acids Res 32 [Database issue]:D35–D40.

Yao PJ, Zhu M, Pyun EI, Brooks AI, Therianos S, Meyers VE, Coleman PD (2003) Defects in expression of genes related to synaptic vesicle trafficking in frontal cortex of Alzheimer's disease. Neurobiol Dis 12:97–109.

Yu H, Saura CA, Choi SY, Sun LD, Yang X, Handler M, Kawarabayashi T, Younkin L, Fedeles B, Wilson MA, Younkin S, Kandel ER, Kirkwood A, Shen J (2001) APP processing and synaptic plasticity in presenilin-1 conditional knockout mice. Neuron 31:713–726.

Zhang P, Hirsch EC, Damier P, Duyckaerts C, Javoy-Agid F (1992) c-*fos* protein-like immunoreactivity: distribution in the human brain and over-expression in the hippocampus of patients with Alzheimer's disease. Neuroscience 46:9–21.